

Performance Analysis for Transmission of Correlated Sources over Non-Orthogonal MARCs

Jiguang He[†], Iqbal Hussain[†], Valtteri Tervo[†], Markku Juntti[†], Tad Matsumoto^{†*}

[†]Centre for Wireless Communications, FI-90014, University of Oulu, Finland

*Japan Advanced Institute of Science and Technology (JAIST) 1-1 Asahidai, Nomi, Ishikawa, 923-1292, Japan

Email: {jhe, iqbal.hussain, valtteri.tervo, markku.juntti}@ee.oulu.fi, matumoto@jaist.ac.jp

Abstract—Non-orthogonal transmission is considered as one of the promising approaches to improve the throughput of current and future wireless communication networks. We focus on the transmission of correlated sources over a non-orthogonal multiple access relay channel (MARC), which consists of two sources, one relay, and one destination. For non-orthogonal transmission over such networks, only two time slots are required as compared to three time slots used in the conventional orthogonal MARC. At the relay node, physical-layer network coding technique is employed to decode the bit-wise exclusive OR (XOR) version of the sources' information sequences rather than decode their original individual information sequences. Subsequently, the relay re-encodes the decoded combined sequence and forwards it to the destination. The destination then exploits this sequence as a helper to recover the sources' original individual information sequences. We analyze the outage probability of the non-orthogonal MARC based on the theorem of multiple access channel (MAC) with a helper, which combines Slepian-Wolf compression rate region and MAC capacity region. Simulation results are provided to verify the accuracy of the theoretical analysis.

I. INTRODUCTION

Cooperation among nodes in wireless cooperative networks is of great importance as it provides diversity gain and coverage extension even with a single antenna at each node. Multiple access relay channel (MARC) is one of the typical wireless cooperative networks and has been well investigated [1]–[6]. In [1], [2], the outage probability of the MARC was formulated under the assumption of orthogonal transmission and perfect intra links (i.e., source-to-relay links). Lu *et al* [3] further relaxed the assumption of error-free intra links and re-formulated the outage probability. Practical joint network-channel coding (JNCC) schemes were investigated in [4]–[6] over MARC using different channel codes, such as low-density parity-check (LDPC) codes [4], [5] and turbo-like codes [6]. However, orthogonal transmission was postulated in all the aforementioned literature.

Due to the low efficiency of the orthogonal transmission, non-orthogonal transmission has recently attracted a lot of attention, for instance, in coded random access [7], [8]. The non-orthogonal transmission of correlated sources over Gaussian multiple access channel (MAC) was investigated in [9].

This work has been performed in the framework of the FP7 project ICT-619555 RESCUE (Links on-the-fly Technology for Robust, Efficient and Smart Communication in Unpredictable Environments), which is partly funded by the European Union. This work is also partially supported by the network compression based wireless cooperative communication systems (NETCOBRA, No. 268209) project, funded by the Academy of Finland.

In many applications, the original information of the sources is not required at the relay. Therefore, the relay does not need to decode the individual information of the sources. Instead, the relay decodes the bit-wise exclusive OR (XOR) version of the sources. We term such MAC as XMAC [10]. In practice, physical-layer network coding (PNC) is widely used for such scenario [11], [12].

We extend the non-orthogonal transmission to the MARC presented in [1]–[3]. The derivation of the closed form expression of the XMAC capacity is very challenging. To facilitate our outage calculations, we introduce an approximated virtual point-to-point (P2P) channel for the XMAC in a heuristic manner. Subsequently, we compare the log-likelihood ratio (LLR) information and the constellation-constrained capacities of the XMAC and the virtual P2P channel by using binary phase-shift keying (BPSK) modulation. We show that the probability density functions (pdfs) of the LLR information of the two channels are quite close to each other. Furthermore, the constellation-constrained capacities of the two channels are also close, especially in the medium and high signal-to-noise ratio (SNR) regimes. We calculate the closed form expression for the capacity of the virtual channel under the assumption of Gaussian signaling and substitute it for the capacity of the XMAC. The outage probability for the MARC is derived based on the non-orthogonal MAC channel consisting of source-to-destination links and a helper (i.e., estimated XOR version of the sources) from the relay. This derivation is based on sufficient conditions. Therefore, the achievable rate region should be smaller than that derived from the necessary conditions. Hence, the outage is an upper bound. However, when designing systems in practice, the use of the upper bound outage provides safer side of service area design. Numerical results are provided to verify the correctness of the theoretical analysis.

II. SYSTEM MODEL

The block diagram of the non-orthogonal MARC is shown in Fig 1. It consists of two sources, one relay, and one destination. Each node is assumed to be equipped with a single antenna and operated in a half-duplex mode. We also assume that there is no cooperation between the sources. The transmission round is divided into two time slots as compared to three time slots consumption in the conventional orthogonal MARC. During the first time slot, the uniform information sequences generated from sources A and B are encoded, modulated, and simultaneously transmitted to the relay and the

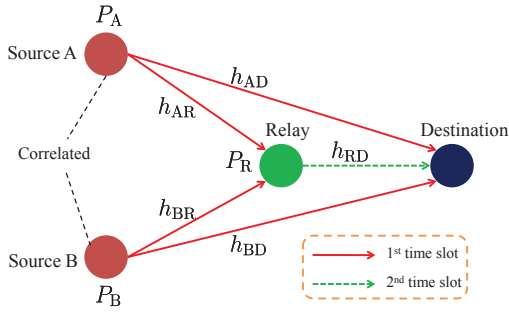


Fig. 1: The block diagram of the non-orthogonal MARC.

destination. Let the modulated symbol sequences of sources A and B be denoted by \mathbf{x}_A and \mathbf{x}_B , respectively. For convenience, we assume that each symbol has unit power. The received signal at the relay and destination during the first time-slot transmission can be expressed as

$$\mathbf{y}_{R,1} = \sqrt{P_A}h_{AR}\mathbf{x}_A + \sqrt{P_B}h_{BR}\mathbf{x}_B + \mathbf{n}_{R,1}, \quad (1)$$

$$\mathbf{y}_{D,1} = \sqrt{P_A}h_{AD}\mathbf{x}_A + \sqrt{P_B}h_{BD}\mathbf{x}_B + \mathbf{n}_{D,1}, \quad (2)$$

where all the wireless links, i.e., h_{AR} , h_{BR} , h_{AD} , and h_{BD} , suffer from independent and identically distributed (i.i.d.) Rayleigh block fading distributed as $\mathcal{CN}(0,1)$, P_i is the transmit power at source i , for $i \in \{A,B\}$, and each entry of additive white Gaussian noise (AWGN) vector $\mathbf{n}_{j,1}$ also follows $\mathcal{CN}(0,1)$, for $j \in \{R,D\}$. The average individual received SNRs can be written by

$$\gamma_{ij} = P_i|h_{ij}|^2, \quad \text{for } i \in \{A,B\} \text{ and } j \in \{R,D\}, \quad (3)$$

where $|h_{ij}|^2$ follows exponential distribution with unit mean and unit variance. The pdf of γ_{ij} can be expressed as

$$p(\gamma_{ij}) = \frac{1}{P_i} \exp(-\frac{\gamma_{ij}}{P_i}), \quad \text{for } i \in \{A,B\} \text{ and } j \in \{R,D\}. \quad (4)$$

Because the relay is not interested in the original information of the sources, the relay directly estimates the bit-wise XOR of the data sequences transmitted by sources A and B. Regardless of the correctness of the estimation, the relay re-encodes and modulates the estimated XOR version to \mathbf{x}_R and forwards it to the destination during the second time slot. The received signal at the destination during the second time-slot transmission is given by

$$\mathbf{y}_{D,2} = \sqrt{P_R}h_{RD}\mathbf{x}_R + \mathbf{n}_{D,2}, \quad (5)$$

where P_R denotes the transmit power at the relay, h_{RD} is the i.i.d. Rayleigh block fading distributed as $\mathcal{CN}(0,1)$, and each entry of $\mathbf{n}_{D,2}$ also follows $\mathcal{CN}(0,1)$.

III. SOURCE-TO-RELAY TRANSMISSION

In this paper, we assume that source A (U_A) and source B (U_B) are correlated, which can be modeled by bit-flipping model,

$$U_A = U_B \oplus U, \quad (6)$$

where $\Pr(U = 1) = p_u$. In this sense, the bit-wise XOR version of U_A and U_B , i.e., $U_{A \oplus B} = U_A \oplus U_B$, has the following probability mass function (pmf) $\Pr(U_{A \oplus B} = 1) = p_u$ and $\Pr(U_{A \oplus B} = 0) = 1 - p_u$.

For the transmission from the sources to the relay, we introduce the concept of PNC at the relay. The estimated bit-wise XOR is treated as a helper for the MAC transmission from the sources to the destination. For the purpose of tractability, the XMAC, shown in (1), is approximated by a virtual P2P channel with transmission of non-uniform/uniform binary i.i.d sources (i.e., $0 \leq p_u \leq 0.5$). The virtual channel is in the form of

$$h = \begin{cases} h_{AR}, & \text{if } |h_{AR}| < |h_{BR}|, \\ h_{BR}, & \text{if } |h_{AR}| \geq |h_{BR}|. \end{cases} \quad (7)$$

Assuming that $P_A = P_B = P$, the received signal for this virtual channel can be written by

$$\mathbf{y}_V = \sqrt{P}h\mathbf{x} + \mathbf{n}, \quad (8)$$

where \mathbf{x} is the modulated symbol sequence of the XOR version of \mathbf{x}_A and \mathbf{x}_B , and each entry of additive noise vector \mathbf{n} follows $\mathcal{CN}(0,1)$. Further details of the virtual channel are given in Appendix A.

The pdf of the average SNR of the virtual channel has been changed into

$$p(\gamma_V) = \frac{2}{P} \exp(-\frac{2\gamma_V}{P}). \quad (9)$$

Referring to the lossy source channel separation theorem [1], [3], we obtain

$$R_D(p_e)R_c \leq C(\gamma_V), \quad (10)$$

where $R_D(\cdot)$ represents the rate distortion function, $C(a) = \log_2(1+a)$ is the capacity function under the assumption of Gaussian signaling, and R_c is the multiplication of channel coding rate and modulation order, i.e., transmission rate, for the virtual P2P channel. Setting $\Phi(\gamma_V) = C(\gamma_V)/R_c$, the calculation of the Hamming distortion for the virtual channel, i.e., p_e , in (10) can be computed by

$$p_e = \begin{cases} H_b^{-1}[H_b(p_u) - \Phi(\gamma_V)], & \text{for } \Phi^{-1}(0) \leq \gamma_V \leq \Phi^{-1}[H_b(p_u)], \\ 0, & \text{for } \gamma_V \geq \Phi^{-1}[H_b(p_u)], \end{cases} \quad (11)$$

where $H_b(p) = -p \log_2(p) - (1-p) \log_2(1-p)$ denotes the binary entropy function, $H_b^{-1}(\cdot)$ denotes its inverse function, and $\Phi^{-1}(a) = 2^{aR_c} - 1$ is the inverse function of $\Phi(\cdot)$. The approximated closed form expression of $H_b^{-1}(\cdot)$ is given in [13]. The relationship between the decoded version of $U_{A \oplus B}$ (denoted by $\hat{U}_{A \oplus B}$) and the original one can also be modeled by bit-flipping model with correlation p_e ,

$$\hat{U}_{A \oplus B} = U_{A \oplus B} \oplus E, \quad (12)$$

where $\Pr(E = 1) = p_e$.

IV. MAC WITH A HELPER

The source-to-destination transmission combined with relay-to-destination transmission can be regarded as MAC with a helper, as shown in Fig. 2. The capacity region is unknown. Instead, we take the intersection of the Slepian-Wolf compression rate region and the MAC capacity region into consideration to obtain an achievable rate region [14]. This derivation is based on the sufficient conditions for lossless communication.

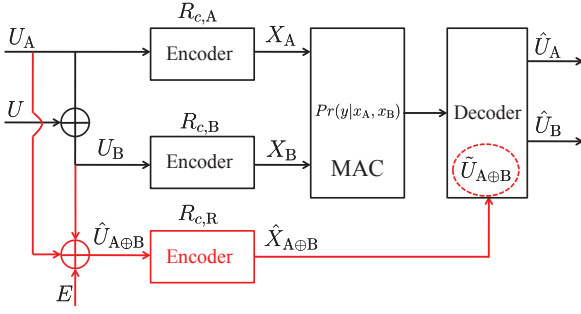


Fig. 2: Illustration of MAC with a helper.

The Slepian-Wolf compression rate region without the helper can be represented by

$$R_{s,A} \geq H(U_A|U_B) = H_b(p_u), \quad (13)$$

$$R_{s,B} \geq H(U_B|U_A) = H_b(p_u), \quad (14)$$

$$R_{s,A} + R_{s,B} \geq H(U_A, U_B) = 1 + H_b(p_u), \quad (15)$$

where $R_{s,A}$ and $R_{s,B}$ are the compression rates of sources A and B, respectively. With the aid of the helper, the Slepian-Wolf compression rate region will be enlarged to

$$\begin{aligned} R_{s,A} &\geq H(U_A|U_B, \tilde{U}_{A\oplus B}) \\ &= H_b(p_u) + H_b(p_e * p_d) - H_b(p_u * p_e * p_d), \end{aligned} \quad (16)$$

$$\begin{aligned} R_{s,B} &\geq H(U_B|U_A, \tilde{U}_{A\oplus B}) \\ &= H_b(p_u) + H_b(p_e * p_d) - H_b(p_u * p_e * p_d), \end{aligned} \quad (17)$$

$$\begin{aligned} R_{s,A} + R_{s,B} &\geq H(U_A, U_B|\tilde{U}_{A\oplus B}) \\ &= 1 + H_b(p_u) + H_b(p_e * p_d) - H_b(p_u * p_e * p_d), \end{aligned} \quad (18)$$

where $\tilde{U}_{A\oplus B}$ is the estimated error version of $\hat{U}_{A\oplus B}$ with correlation p_d at the destination and $a*b = a(1-b) + (1-a)b$. The relationship between $\tilde{U}_{A\oplus B}$ and $\hat{U}_{A\oplus B}$ can be modeled by

$$\tilde{U}_{A\oplus B} = \hat{U}_{A\oplus B} \oplus D, \quad (19)$$

where $\Pr(D = 1) = p_d$. Similar to (11), p_d can be calculated as

$$p_d = \begin{cases} H_b^{-1}[H_b(p_u * p_e) - \Phi(\gamma_{R,D})], & \text{for } \Phi^{-1}(0) \leq \gamma_{R,D} \leq \Phi^{-1}[H_b(p_u * p_e)], \\ 0, & \text{for } \gamma_{R,D} \geq \Phi^{-1}(H_b(p_u * p_e)). \end{cases} \quad (20)$$

More details on derivation of (16)–(18) can be found in [1], [3].

According to the lossless source channel separation theorem, the MAC capacity region is determined by

$$R_{s,A}R_{c,A} \leq C(\gamma_{A,D}), \quad (21)$$

$$R_{s,B}R_{c,B} \leq C(\gamma_{B,D}), \quad (22)$$

$$R_{s,A}R_{c,A} + R_{s,B}R_{c,B} \leq C(\gamma_{A,D} + \gamma_{B,D}), \quad (23)$$

where $R_{c,A}$ and $R_{c,B}$ are the transmission rates of sources A and B, respectively. The achievable rate region is the intersection part determined by (16)–(18) and (21)–(23).

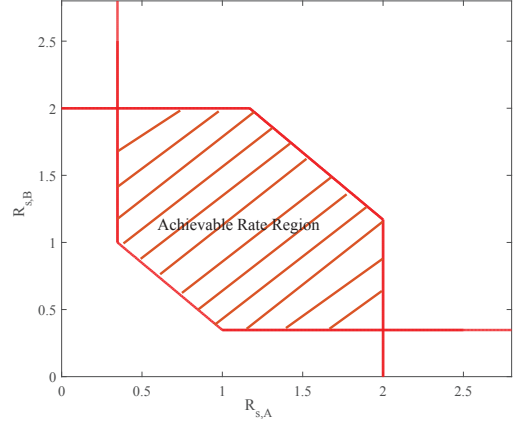


Fig. 3: The achievable rate region for the MAC with a helper.

A. An Example

Let's show a detailed example to illustrate the achievable rate region. We set $R_{c,A} = R_{c,B} = 1/2$, $p_u = p_e = p_d = 0.1$, and $\gamma_{A,D} = \gamma_{B,D} = 0$ dB. The achievable rate region is shown in Fig. 3. The achievable rate region is affected by many factors such as the values of $R_{c,A}$, $R_{c,B}$, P , p_u , p_e , and p_d . We mainly focus on the factors p_e and p_d , which are determined by the XMAC channel and the relay-to-destination link.

B. Outage Probability

For simplicity, we assume the same transmission rate for the two sources, i.e., $R_{c,A} = R_{c,B} = R_c$. Consequently, we define the event of successful transmission as

$$\begin{aligned} \mathcal{S} = \{ & H_b(p_u) + H_b(p_e * p_d) - H_b(p_u * p_e * p_d) \leq C(\gamma_{A,D})/R_c \\ & \wedge H_b(p_u) + H_b(p_e * p_d) - H_b(p_u * p_e * p_d) \leq C(\gamma_{B,D})/R_c \\ & \wedge 1 + H_b(p_u) + H_b(p_e * p_d) - H_b(p_u * p_e * p_d) \leq C(\gamma_{A,D} + \gamma_{B,D})/R_c \}, \end{aligned} \quad (24)$$

where \wedge denotes logical “and” operation. Therefore, the outage probability can be expressed as

$$P_{\text{out}} = 1 - \Pr\{\mathcal{S}\}. \quad (25)$$

Because the derived achievable rate region for the MAC with a helper is smaller than its actual capacity region, the outage probability is correspondingly an upper bound.

Depending on the success or failure of source-to-relay XMAC and relay-to-destination channel, we can rewrite the $\Pr\{\mathcal{S}\}$ in (25) as

$$\Pr\{\mathcal{S}\} = \sum_{i=1}^4 \Pr\{\mathcal{S}|\mathcal{C}_i\}\Pr\{\mathcal{C}_i\}, \quad (26)$$

where

$$\begin{aligned} \mathcal{C}_1 &= \{p_e = 0 \wedge p_d = 0\}, \\ \mathcal{C}_2 &= \{p_e = 0 \wedge p_d \neq 0\}, \\ \mathcal{C}_3 &= \{p_e \neq 0 \wedge p_d = 0\}, \\ \mathcal{C}_4 &= \{p_e \neq 0 \wedge p_d \neq 0\}. \end{aligned} \quad (27)$$

All of the above four events will be transferred into different intervals of a two-dimensional vector consisting of γ_V , $\gamma_{R,D}$. In addition to the effect of direct links from sources to

destination, i.e., $\gamma_{A,D}$ and $\gamma_{B,D}$, the probability of successful transmission $\Pr\{\mathcal{S}\}$ can be calculated by four-fold integrals, i.e.,

$$\Pr\{\mathcal{S}|\mathcal{C}_i\}\Pr\{\mathcal{C}_i\} = \iiint\limits_{\mathbb{V}_i} p(\gamma_V)p(\gamma_{R,D})p(\gamma_{A,D})p(\gamma_{B,D}) d\gamma_V d\gamma_{R,D} d\gamma_{A,D} d\gamma_{B,D}, \quad (28)$$

where

$$\begin{aligned} \mathbb{V}_1 &= \{\gamma_{A,D} \geq \Phi^{-1}(0) \wedge \gamma_{B,D} \geq \Phi^{-1}(0) \\ &\wedge \gamma_{A,D} + \gamma_{B,D} \geq \Phi^{-1}(1), \\ &\wedge \gamma_V \geq \Phi^{-1}[H_b(p_u)] \wedge \gamma_{R,D} \geq \Phi^{-1}[H_b(p_u)]\}, \end{aligned} \quad (29)$$

$$\begin{aligned} \mathbb{V}_2 &= \{\gamma_{A,D} \geq \Phi^{-1}[H_b(p_u) + H_b(p_d) - H_b(p_u * p_d)] \\ &\wedge \gamma_{B,D} \geq \Phi^{-1}[H_b(p_u) + H_b(p_d) - H_b(p_u * p_d)] \wedge \\ &\gamma_{A,D} + \gamma_{B,D} \geq \Phi^{-1}[1 + H_b(p_u) + H_b(p_d) - H_b(p_u * p_d)] \\ &\wedge \gamma_V \geq \Phi^{-1}[H_b(p_u)] \wedge \Phi^{-1}(0) \leq \gamma_{R,D} \leq \Phi^{-1}[H_b(p_u)]\}, \end{aligned} \quad (30)$$

$$\begin{aligned} \mathbb{V}_3 &= \{\gamma_{A,D} \geq \Phi^{-1}[H_b(p_u) + H_b(p_e) - H_b(p_u * p_e)] \\ &\wedge \gamma_{B,D} \geq \Phi^{-1}[H_b(p_u) + H_b(p_e) - H_b(p_u * p_e)] \wedge \\ &\gamma_{A,D} + \gamma_{B,D} \geq \Phi^{-1}[1 + H_b(p_u) + H_b(p_e) - H_b(p_u * p_e)] \wedge \\ &\Phi^{-1}(0) \leq \gamma_V \leq \Phi^{-1}[H_b(p_u)] \wedge \gamma_{R,D} \geq \Phi^{-1}[H_b(p_u * p_e)]\}, \end{aligned} \quad (31)$$

$$\begin{aligned} \mathbb{V}_4 &= \{\gamma_{A,D} \geq \Phi^{-1}[H_b(p_u) + H_b(p_e * p_d) - H_b(p_u * p_e * p_d)] \\ &\wedge \gamma_{B,D} \geq \Phi^{-1}[H_b(p_u) + H_b(p_e * p_d) - H_b(p_u * p_e * p_d)] \wedge \\ &\gamma_{A,D} + \gamma_{B,D} \geq \Phi^{-1}[1 + H_b(p_u) + H_b(p_e * p_d) - H_b(p_u * p_e * p_d)] \\ &\wedge \Phi^{-1}(0) \leq \gamma_V \leq \Phi^{-1}[H_b(p_u)] \\ &\wedge \Phi^{-1}(0) \leq \gamma_{R,D} \leq \Phi^{-1}[H_b(p_u * p_e)]\}. \end{aligned} \quad (32)$$

V. SIMULATION RESULTS

In this section, we draw the theoretical results in terms of the outage probability over the non-orthogonal MARC and compare them to the corresponding Monte Carlo computer simulations. Practical simulations using turbo codes are left for future investigation. The case of perfect intra links from [1] is considered as a benchmark scheme. All the transmission rates are set to be 0.5. The correlation of the sources ranges from 0 to 0.5, which includes transmission of independent sources as well. We assume that the transmit power has the following relationship: $P_A = P_B = P_R$. The simulation results are provided in Fig. 4, where ‘‘Theo’’ represents the theoretical results of the outage probability for the non-orthogonal MARC given by (25), ‘‘MC’’ represents the Monte Carlo simulation results of the outage probability for the non-orthogonal MARC given by (16)–(18) and (21)–(23), and ‘‘Theo [1]’’ represents the theoretical results of the outage probability for the orthogonal MARC from [1] with error-free intra links. Compared to the case in [1], the performance loss is very limited for the non-orthogonal MARC with imperfect intra links, especially when the correlation of the sources is high. Second order diversity can be achieved for all the levels of correlation. As shown in Fig. 4, the Monte Carlo simulations closely approximate the theoretical analysis.

VI. CONCLUSION

We have calculated the outage probability for the transmission of correlated sources over non-orthogonal fading MARC, which is based on the sufficient condition of lossless

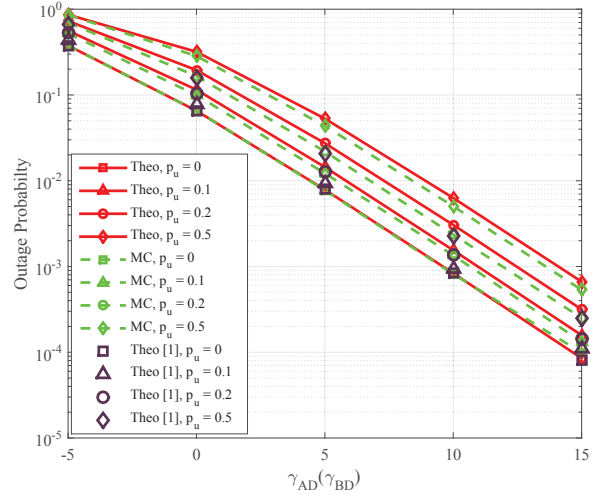


Fig. 4: Outage probabilities of the non-orthogonal MARC for different SNRs.

communication over MAC with the aid of a helper. For the purpose of tractability, first hop transmission from sources to the relay has been represented by an approximated virtual P2P channel validated through intensive numerical simulations. Subsequently, the closed form expression of the capacity for the considered XMAC has been derived using the approximated virtual channel. Finally, it has been shown that the performance results of the non-orthogonal MARC approach its orthogonal counterpart with perfect intra links.

APPENDIX A

VIRTUAL CHANNEL REPRESENTATION

The received signal from the XMAC channel is shown in (1). Assuming that BPSK modulation is applied for the XMAC channel. Then, the LLR information of the XMAC channel can be expressed as

$$L_X = \ln \left(\frac{\exp(-|y_{R,1} - \sqrt{P}(h_{AR} + h_{BR})|^2) + \exp(-|y_{R,1} - \sqrt{P}(h_{AR} - h_{BR})|^2)}{\exp(-|y_{R,1} + \sqrt{P}(h_{AR} + h_{BR})|^2) + \exp(-|y_{R,1} + \sqrt{P}(h_{AR} - h_{BR})|^2)} \right), \quad (33)$$

where $|\cdot|$ denotes the absolute value. Similarly, the LLR information for the virtual channel can be expressed as

$$L_V = \ln \left(\exp(-|y_V - \sqrt{P}h|^2) / \exp(-|y_V + \sqrt{P}h|^2) \right). \quad (34)$$

The performance of the relay is mainly determined by the iterative decoder. From decoding perspective, the only difference between the XMAC and the virtual channel is the input from channel to the decoder. Therefore, we investigate the output LLRs of both channels. As observed from Fig. 5, the pdfs of L_X and L_V are quite similar, especially in medium and high SNR regimes.

The constellation-constrained capacities of the XMAC and the virtual channel under the constraint of BPSK modulation are shown in Fig. 6. The constellation-constrained capacity of the P2P fading channel (e.g., $h = h_{AR}$ in (8)) is given as a benchmark scheme. As shown in the figure, the constellation-constrained capacities of the XMAC and the virtual channel

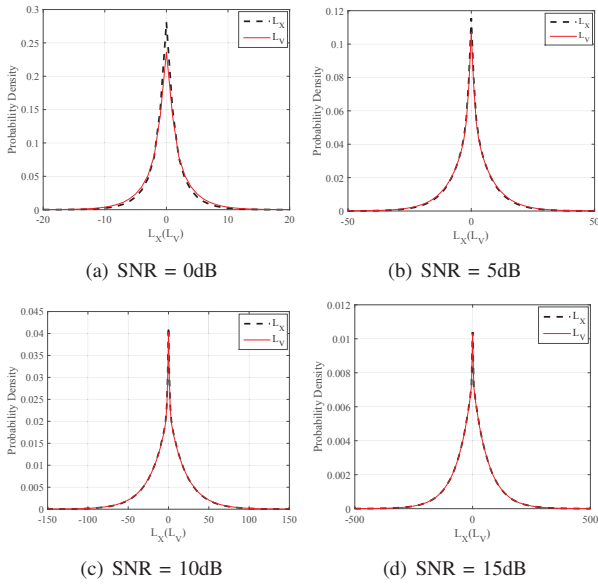


Fig. 5: Pdfs of L_X and L_V .

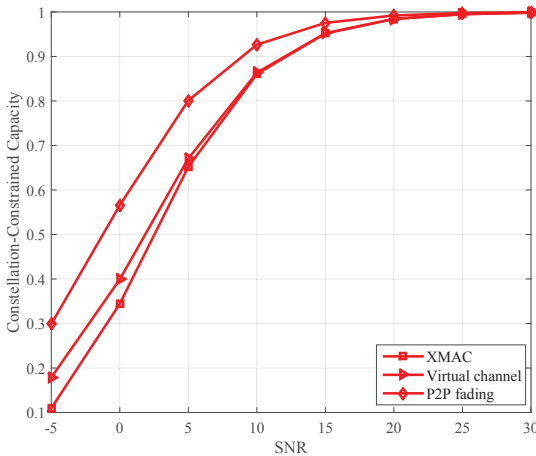


Fig. 6: Constellation-constrained capacities of the XMAC and the virtual channel under BPSK modulation.

are also very close to each other, especially in medium and high SNR regimes.

To further confirm the accuracy of the approximation of the two channels, we run practical simulations using rate-1/2 ACC aided turbo code [15] for the XMAC channel and evaluate the frame error rate (FER) performance. Moreover, we calculate the theoretical outage probability based on the virtual channel. The simulation results are provided in Fig. 7. The performance gap is within 4 dB for all the levels of correlation.

Therefore, we can conclude that the XMAC channel and the virtual channel are closely approximated. Consequently, the capacity of the virtual channel under the constraint of Gaussian signaling can be simplified by

$$C_V = \log_2(1 + P|h|^2), \quad (35)$$

where $|h|^2$ also follows exponential distribution, i.e., $p(|h|^2) = 2\exp(-2|h|^2)$. It is straightforward to show that the corresponding average SNR of the virtual channel follows (9).

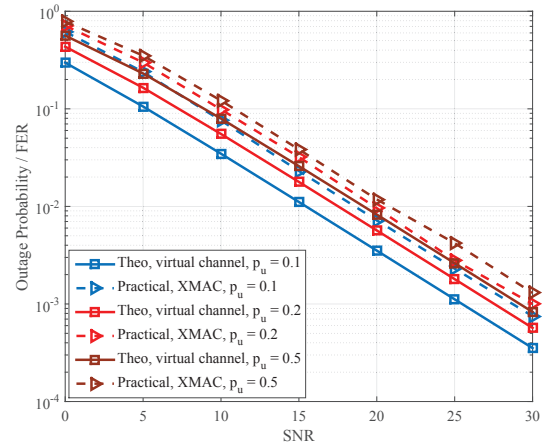


Fig. 7: Comparison between theoretical outage probability of the virtual channel and FER of the XMAC using practical ACC aided turbo code.

REFERENCES

- [1] X. Zhou, P.-S. Lu, K. Anwar, and T. Matsumoto, "Correlated sources transmission in orthogonal multiple access relay channel: Theoretical analysis and performance evaluation," *IEEE Trans. Wireless Commun.*, vol. 13, no. 3, pp. 1424–1435, Mar. 2014.
- [2] D. H. Woldegebreal and H. Karl, "Multiple-access relay channel with network coding and non-ideal source-relay channels," in *Proc. of ISWCS*, Oct. 2007, pp. 732–736.
- [3] P.-S. Lu, X. Zhou, and T. Matsumoto, "Outage probabilities of orthogonal multiple-access relaying techniques with imperfect source-relay links," *IEEE Trans. Wireless Commun.*, vol. 14, no. 4, pp. 2269–2280, Apr. 2015.
- [4] Y. Li, G. Song, and L. Wang, "Design of joint network-low density parity check codes based on the EXIT charts," *IEEE Commun. Lett.*, vol. 13, no. 8, pp. 600–602, Aug. 2009.
- [5] S. Schwandtner, A. G. i. Amat, and G. Matz, "Spatially-coupled LDPC codes for decode-and-forward relaying of two correlated sources over the BEC," *IEEE Trans. Commun.*, vol. 62, no. 4, pp. 1324–1337, Apr. 2014.
- [6] R. Youssef and A. G. i. Amat, "Distributed serially concatenated codes for multi-source cooperative relay networks," *IEEE Trans. Wireless Commun.*, vol. 10, no. 1, pp. 253–263, Jan. 2011.
- [7] E. Paolini, C. Stefanovic, G. Liva, and P. Popovski, "Coded random access: applying codes on graphs to design random access protocols," *IEEE Commun. Mag.*, vol. 53, no. 6, pp. 144–150, Jun. 2015.
- [8] Z. Zhang, C. Xu, and L. Ping, "Coded random access with distributed power control and multiple-packet reception," *IEEE Wireless Commun. Lett.*, vol. 4, no. 2, pp. 117–120, Apr. 2015.
- [9] J. He, I. Hussain, M. Juntti, and T. Matsumoto, "Transmission of correlated sources over non-orthogonal Gaussian MACs," in *Proc. of IEEE ICC workshop*, May. 2016.
- [10] J. Kim and W. E. Stark, "Error exponent of exclusive-or multiple-access channels," in *Proc. of IEEE ISIT*, Jun. 2009, pp. 1709–1713.
- [11] P. Popovski and H. Yomo, "Physical network coding in two-way wireless relay channels," in *Proc. of IEEE ICC*, Jun. 2007, pp. 707–712.
- [12] S. Zhang and S. C. Liew, "Channel coding and decoding in a relay system operated with physical-layer network coding," *IEEE J. Sel. Areas Commun.*, vol. 27, no. 5, pp. 788–796, Jun. 2009.
- [13] X. Zhou, M. Cheng, X. He, and T. Matsumoto, "Exact and approximated outage probability analyses for decode-and-forward relaying system allowing intra-link errors," *IEEE Trans. Wireless Commun.*, vol. 13, no. 12, pp. 7062–7071, Dec. 2014.
- [14] T. M. Cover and J. A. Thomas, *Elements of Information Theory 2nd Edition*. New York, NY, USA: Wiley, 2006.
- [15] K. Anwar and T. Matsumoto, "Accumulator-assisted distributed turbo codes for relay systems exploiting source-relay correlation," *IEEE Commun. Lett.*, vol. 16, no. 7, pp. 1114–1117, Jul. 2012.